PLXNA4 Is Associated with Alzheimer Disease and Modulates Tau Phosphorylation

Gyungah Jun, PhD,[1,2,3] Hirohide Asai, MD, PhD,[4] Ella Zeldich, PhD,[5] Elodie Drapeau, PhD,[6] CiDi Chen, PhD,[5] Jaeyoon Chung, MS,[1] Jong-Ho Park, MS,[7] Sehwa Kim, MS,[7] Vahram Haroutunian, MD,[6] Tatiana Foroud, PhD,[8] Ryozo Kuwano, MD, PhD,[9] Jonathan L. Haines, PhD,[10] Margaret A. Pericak-Vance, PhD,[11] Gerard D. Schellenberg, PhD,[12] Kathryn L. Lunetta, PhD,[3] Jong-Won Kim, MD, PhD,[7,13] Joseph D. Buxbaum, PhD,[6] Richard Mayeux, MD,[14] Tsuneya Ikezu, MD, PhD,[4,15] Carmela R. Abraham, PhD,[4,5] and Lindsay A. Farrer, PhD[1,2,3,15,16]

Objective: Much of the genetic basis for Alzheimer disease (AD) is unexplained. We sought to identify novel AD loci using a unique family-based approach that can detect robust associations with infrequent variants (minor allele frequency < 0.10).

Methods: We conducted a genome-wide association study in the Framingham Heart Study (discovery) and NIA-LOAD (National Institute on Aging–Late-Onset Alzheimer Disease) Study (replication) family-based cohorts using an approach that accounts for family structure and calculates a risk score for AD as the outcome. Links between the most promising gene candidate and AD pathogenesis were explored *in silico* as well as experimentally in cell-based models and in human brain.

Results: Genome-wide significant association was identified with a *PLXNA4* single nucleotide polymorphism (rs277470) located in a region encoding the semaphorin-3A (SEMA3A) binding domain (meta-analysis *p* value [meta-P] $= 4.1 \times 10^{-8}$). A test for association with the entire region was also significant (meta-P $= 3.2 \times 10^{-4}$). Transfection of SH-SY5Y cells or primary rat neurons with full-length PLXNA4 (TS1) increased tau phosphorylation with stimulated by SEMA3A. The opposite effect was observed when cells were transfected with shorter isoforms (TS2 and TS3). However, transfection of any isoform into HEK293 cells stably expressing amyloid β (Aβ) precursor protein (APP) did not result in differential effects on APP processing or Aβ production. Late stage AD cases (n = 9) compared to controls (n = 5) had 1.9-fold increased expression of TS1 in cortical brain tissue ($p = 1.6 \times 10^{-4}$). Expression of TS1 was

View this article online at wileyonlinelibrary.com. DOI: 10.1002/ana.24219

Received Apr 13, 2014, and in revised form Jul 2, 2014. Accepted for publication Jul 2, 2014.

Address correspondence to Dr Farrer, Biomedical Genetics E200, Boston University School of Medicine, 72 East Concord Street, Boston, MA 02118. E-mail: farrer@bu.edu

From the Departments of [1]Medicine and [2]Ophthalmology, Boston University School of Medicine, Boston, MA; [3]Department of Biostatistics, Boston University School of Public Health, Boston, MA; [4]Department of Pharmacology and Experimental Therapeutics, Boston University School of Medicine, Boston, MA; [5]Department of Biochemistry, Boston University School of Medicine, Boston, MA; [6]Department of Psychiatry and Friedman Brain Institute, Icahn School of Medicine at Mount Sinai, New York, NY; [7]Department of Health Sciences and Technology, Graduate School, Samsung Advanced Institute for Health Science and Technology, Seoul, Korea; [8]Department of Medical and Molecular Genetics, Indiana University School of Medicine, Indianapolis, IN; [9]Department of Molecular Genetics, Brain Research Institute, Niigata University, Niigata, Japan; [10]Department of Epidemiology and Biostatistics, Case Western Reserve University, Cleveland, OH; [11]John P. Hussman Institute for Human Genomics, University of Miami, Miami, FL; [12]Department of Pathology and Laboratory Medicine, University of Pennsylvania School of Medicine, Philadelphia, PA; [13]Department of Laboratory Medicine and Genetics, Samsung Medical Center, Sungkyunkwan University School of Medicine, Seoul, Korea; [14]Department of Neurology and Taub Institute, Columbia University, New York, NY; [15]Department of Neurology, Boston University School of Medicine, Boston, MA; and [16]Department of Epidemiology, Boston University School of Public Health, Boston, MA.

Additional Supporting Information may be found in the online version of this article.

significantly correlated with the Clinical Dementia Rating score ($\rho = 0.75$, $p = 2.2 \times 10^{-4}$), plaque density ($\rho = 0.56$, $p = 0.01$), and Braak stage ($\rho = 0.54$, $p = 0.02$).
Interpretation: Our results indicate that PLXNA4 has a role in AD pathogenesis through isoform-specific effects on tau phosphorylation.

ANN NEUROL 2014;76:379–392

Alzheimer disease (AD) is the most frequent age-related dementia, affecting 5.4 million Americans, including 13% of people aged 65 years and older and >40% of people aged 85 years and older.[1] Genetic factors account for much of the risk for developing AD, with heritability estimates between 60% and 80%.[2] The apolipoprotein E (*APOE*) ε4 allele is a well-recognized major risk factor for late onset AD, increasing the odds of disease in a dose-dependent fashion.[3] Common polymorphisms in 19 additional genes have been robustly established as risk factors for AD using large-scale genome-wide association studies (GWASs) and meta-analyses.[4] These polymorphisms link to mechanisms of Aβ metabolism, lipid metabolism, inflammation, and axon guidance.[5,6] However, the heritability of AD explained by *APOE* is <30%, and by each of the novel GWAS loci is <1%, suggesting that <50% of the genetic contribution to AD is explained by known common polymorphisms.[4,7,8] The remaining heritability may be due to additional common variants of weaker effect, rare variants, copy-number variants, insertion–deletion polymorphisms, and gene–gene and gene–environment interactions.[9,10]

Here, we conducted a 2-stage family-based AD GWAS using a novel method that incorporates the entire family structure and reduces diagnostic misclassification in the association test, and renders a result that is less prone to type I error, even for rare variants.[11] We obtained strong evidence of association in the Framingham Heart Study (FHS) data set with several single nucleotide polymorphisms (SNPs) in *PLXNA4*, a gene that had not been previously linked to AD. Several other *PLXNA4* SNPs were highly significant in the National Institute on Aging–Late-Onset Alzheimer Disease (NIA-LOAD) Study data set. Subsequent in silico and molecular studies demonstrated isoform-specific effects of PLXNA4 on hyperphosphorylation of tau protein, a terminal step leading to breakdown of neuronal signaling and microtubule formation.

Subjects and Methods

Study Cohorts

FHS DISCOVERY COHORT. The FHS is a multigenerational study of health and disease in a prospectively followed community-based sample. Details on procedures for assessing dementia and determining AD status in this cohort are described elsewhere.[12] We included only incident AD cases who had a magnetic resonance imaging scan prior to disease onset. Clinical, demographic, genetic, and pedigree information were obtained from dbGaP (http://www.ncbi.nlm.nih.gov/gap). Phenotypic and GWAS data were available for 61 cases and 2,530 cognitively normal controls from 1,232 families. This sample contained 287 parent–offspring pairs, 1,215 sib pairs, 236 avuncular pairs, 714 cousin pairs, and 436 spouse pairs. The 61 AD cases are members of 57 families, and 3 of these families contained distantly related affected individuals included in the analyses. Sixteen families did not have any genotyped AD cases but contained individuals with a history of dementia.

NIA-LOAD REPLICATION COHORT. The NIA-LOAD Study recruited families with ≥2 affected members available for genotyping.[13] Phenotype and GWAS data for this cohort were obtained from dbGaP. The GWAS data set included a total of 1,819 AD cases and 1,969 unaffected individuals from 2,265 families. The 1,819 AD cases are distributed among 988 families containing 1,010 concordantly affected, 878 discordantly affected, and 541 concordantly unaffected sib pairs. Within the GWAS data set, there were 526 parent–offspring pairs, 2,429 sib pairs, 1,905 avuncular pairs, 1,533 cousin pairs, and 28 spouse pairs.

ALZHEIMER'S DISEASE GENETICS CONSORTIUM REPLICATION COHORT. We obtained summarized results for SNPs located in the top-ranked locus from each of the individual Alzheimer's Disease Genetics Consortium (ADGC) data sets (excluding the NIA-LOAD data set), which are described elsewhere.[7,14,15] This sample included 18,901 Caucasians (9,966 cases and 8,935 controls), 4,896 African Americans (1,459 cases and 3,437 controls), and 1,845 Japanese (951 cases and 894 controls).

Genotyping, Quality Control, Population Substructure, and Imputation

FHS samples were genotyped at Affymetrix (Santa Clara, CA) using the Affymetrix GeneChip Human Mapping 500K Array Set and 50K Human Gene Focused Panel.[16] NIA-LOAD samples were genotyped using Illumina (San Diego, CA) 610 high-density SNP microarrays.[7] *APOE* genotypes were obtained by restriction fragment length polymorphism analysis for the FHS cohort and by haplotype analysis of SNPs rs7412 and rs429358, which were genotyped at Prevention Genetics (http://www.preventiongenetics.com) for the NIA-LOAD cohort.

Quality control (QC) procedures and analysis of population substructure were performed as previously described.[17] In the discovery genome-wide association data set, 341,492 SNPs genotyped in 2,591 subjects passed QC. Based on this number

of SNPs, the threshold for genome-wide significance was $p = 1.46 \times 10^{-7}$.

In candidate gene analyses in the FHS and NIA-LOAD data sets, we evaluated SNPs within 50kb of the top-ranked gene from the discovery GWAS that were imputed previously using the HapMap 2 CEU reference panel and the MaCH program.[17,18] SNPs with an imputation quality measure (R^2) < 0.80 were excluded.

Statistical Analysis

AD RISK SCORES. We calculated AD risk scores using 2 different approaches. In the FHS data set, liability scores are residuals from a logistic regression model for AD affection status adjusting for sex and censoring age (age at onset of AD or age at examination of controls) evaluated using R.[17] We did not adjust for previously derived principal components (PCs) of population substructure because they were not significantly associated with the liability scores in the FHS data set.[19] In the NIA-LOAD data set, we calculated liability scores (residuals) from a logistic regression model for AD affection status adjusting for sex, censoring age, and including the first 2 genotype-covariance matrix PCs to account for population substructure. We also computed propensity scores in the NIA-LOAD data set to account for the approximately 10-year lower mean age of in this cohort compared to the FHS cohort and ascertainment of families with multiple affected members. This method was suggested previously for analysis of a binary trait with various ages at onset and examination among affected and unaffected subjects, respectively.[20,21] Propensity scores were obtained for unaffected family members using the AGEON program in S.A.G.E. (v6.2)[22] as the probability of getting disease conditioned on affection status and censoring ages of their parents. Affection status for AD cases (probability = 1) was retained in the model. Propensity scores were further adjusted for censoring age, sex, and the first 2 PCs in a linear regression model, and the residuals were used as the outcome variable. We were unable to obtain propensity scores in the FHS data set because of incomplete parental information.

SNP ASSOCIATION TEST. The quantitative risk scores (residuals from liability or propensity scores) were normalized by taking the inverse standard normal transformation of the empirical quantile that was obtained using the formula $r(y) - 1/3$ divided by $n + 1/3$, where $r(y)$ is the rank of residuals, y. This approach has been demonstrated to be valid for family-based association tests even for a binary trait with rare variants.[23] Association of the normalized risk scores with each SNP was evaluated using the extension of the 2-level Haseman–Elston regression method implemented in the RELPAL program in S.A.G.E. (v6.1).[24,25] Models included a term for an inheritance vector of exhaustive relative pairs. Nominal probability values for association were determined using first-level Wald tests. For top-ranked genes, we conducted association tests for genotyped and well-imputed SNPs ($R^2 \geq 0.8$) in the FHS and the NIA-LOAD data sets using a risk score (ie, liability score or propensity score) as a quantitative trait.

REGIONAL ASSOCIATION TEST. To allow for the possibility of allelic heterogeneity between the 2 family data sets, we performed association tests within each data set for regions in the top-ranked gene defined by the ligand-binding domain of the encoded protein using the VEGAS (Versatile Gene-Based Association Study) program, which calculates probability values based on 100,000 permutations.[26]

META-ANALYSIS. Results from the FHS and NIA-LOAD data sets were combined by meta-analysis of Z scores weighted by the number of subjects using METAL.[27] In region-based meta-analysis, we assumed the same direction of effect on a region in both data sets and combined results using the Z score approach. The summary results for the ADGC data sets (excluding the NIA-LOAD Study) were meta-analyzed using the inverse variance method in METAL after applying a genomic control within each individual data set.[7]

Amyloid β Precursor Protein and Amyloid β Analyses

CELL MAINTENANCE AND TRANSFECTION. HEK293 cells stably transfected with wild-type APP751 were maintained as previously described.[28] The day before transfection, cells were split into 6-well plates at a density of 1×10^5 cells per well. The cells were transfected with empty vector (EV) or PLXNA4 isoforms (TS1, TS2, or TS3) from OriGene using Attractene (Qiagen, Valencia, CA). Forty-eight hours post-transfection, media were collected and cells were lysed as described.[28]

SODIUM DODECYL SULFATE–POLYACRYLAMIDE GEL ELECTROPHORESIS AND WESTERN BLOTTING. Proteins were separated on 8% Tris–glycine gels and transferred onto nitrocellulose (Millipore, Billerica, MA). Primary antibodies were mouse monoclonal 6E10 (1:1,000; Covance, Princeton, NJ) against amino acids 1 to 17 of amyloid β (Aβ), which also recognize full-length Aβ precursor protein (APP) and APPsα, anti-Myc monoclonal antibody (MAb; 1:1,000; Sigma, St Louis, MO), and mouse monoclonal β-tubulin (1:10,000; Invitrogen, Carlsbad, CA). Secondary antibody was peroxidase-labeled goat antimouse immunoglobulin G (IgG; 1:500; KPL, Gaithersburg, MD). The Supersignal West Pico Chemiluminescent Substrate (Thermo Scientific, Waltham, MA) was used for detection. Protein expression was analyzed by densitometry using ImageJ (NIH shareware program). The expression of APPsα was normalized to total APP.

Aβ ENZYME-LINKED IMMUNOSORBENT ASSAY. Forty-eight hours after transfection of HEK293 cells (stably transfected with wtAPP751) with EV or PLXNA4 isoforms (TS1, TS2, or TS3), media were collected and centrifuged at 16,873 $\times$ g for 5 minutes at 4°C to discard cell debris. Enzyme-linked immunosorbent assays (ELISAs) were carried out using the human Aβ40 and Aβ42 ELISA kits (Invitrogen) in accordance with manufacturer's protocol with samples diluted 1:2 in diluent buffer and as previously described.[28]

Tau Analyses

TAU IMMUNOBLOTTING. SH-SY5Y cells (2×10^6) stably expressing mutant tau P301L (SH-SY5Y P301L) were transfected with 1μg of various plexin-A4-Myc or pcDNA3 vectors by Lipofectamine 2000 (Invitrogen). After transfection, cells were treated with or without 3nM Semaphorin3A (Sema3A-FC; R&D Systems, Minneapolis, MN) for 1 hour. Twenty grams of whole cell lysate was immunoblotted with phospho-tau (AT-8, 1:500), total-tau (Tau46, 1:500), β-actin (1:1,000), or Myc (9E10, 1:1,000) as previously described.[29]

PULL-DOWN ASSAY. Plexin-A4-Myc–transfected SH-SY5Y P301L cells were treated with 3nM 6xHis human Sema3A-FC in DMEM/F12/B-27 medium. After Sema3A-FC stimulation, the media were collected and the Sema3A-FC was precipitated with protein A/G agarose, followed by immunoblotting of the samples for Myc (9E10, for detection of plexin-A4 molecules) and 6xHis (H-3, for detection of Sema3A, 1:1,000 Santa Cruz Biotechnology, Santa Cruz, CA).

PRIMARY NEURON CULTURE AND TAU IMMUNOFLUORESCENCE. Rat primary hippocampal neurons were harvested from E18 embryonic brain, plated on poly-D-lysine–coated coverslips, cultured for 14 days, and transfected with full-length or short isoforms of human plexin-A4-Myc DNA plasmid vectors by Lipofectamine 2000 (Invitrogen). Twenty-four hours after transfection, cells were treated with or without 3nM Sema3A-FC for 1 hour, fixed with 4% paraformaldehyde, and costained with T514 phosphorylated collapsing response mediator protein 2 (pT514 CRMP2, Ab62478, rabbit polyclonal, 1:500; Abcam, Cambridge, MA) and β3-tubulin (mouse monoclonal 1:500; Promega, Madison, WI), or costained with AT8 (mouse monoclonal, 1:500) and anti-Myc (rabbit polyclonal, 1:200; Covance), followed by incubation with antimouse IgG Alexa 568–conjugated goat secondary antibody (1:600; Invitrogen) and antirabbit IgG Alexa 488–conjugated goat secondary antibody (1:600, Invitrogen). Immunostained AT8 signals were digitally captured using an inverted fluorescence microscope (TE-2000U; Nikon Instruments, Melvin, NY) and quantified by ImageJ. Data were obtained from at least 100 cells in 3 independent experiments.

Analyses of Gene Expression in Brain

Gene expression experiments were conducted on brain tissue specimens obtained from 19 autopsied subjects including 5 controls (Braak stage 0), 5 early stage AD cases (Braak stages 1–2), and 9 late stage AD cases (Braak stages 3–4). Ascertainment, cognitive assessment, neuropathological assessment, and stratification of these subjects were previously described.[30] Frozen postmortem brain tissue specimens from Brodmann area 9 of subjects were obtained from the Mount Sinai/Bronx Veterans Administration (VA) Medical Center/Department of Psychiatry Brain Bank. Normal controls had no history of any psychiatric or neurological disorders and no discernible neuropathological lesions. The institutional review boards of Pilgrim Psychiatric Center, the Icahn School of Medicine at Mount Sinai, and the Bronx VA Medical Center approved all assessment and postmortem procedures.

Total RNA was isolated from 50mg of tissue by using the Qiagen miRNeasy kit. Isolated RNA samples were treated with 40 units of DNase I (Ambion, Austin, TX) to remove genomic DNA contamination. Template RNA quantity and quality, including degradation, were determined on an Agilent 2100 Bioanalyzer (Agilent Technologies, Santa Clara, CA). Two samples with very low RNA integrity number were excluded from the study. After cDNA synthesis using a Superscript III first-strand synthesis kit (Invitrogen), quantitative polymerase chain reactions (PCRs) were run on an ABI (Foster City, CA) 7900HT real-time machine in triplicate using Platinum Quantitative PCR SuperMix-UDG (Invitrogen) for primers designed with the Roche (Basel, Switzerland) Universal ProbeLibrary or SYBR GreenER qPCR supermix for regular primers for ABI PRISM (Invitrogen). Acquired data were loaded onto qBase v1.3.5 software for QC and normalization to reference genes *GAPDH* and *RPL13A*.

Group differences between TS1 and TS3 or between controls and AD cases were evaluated using analysis of variance and the appropriate *t* test after checking for equality of variances. Pearson correlations were calculated using the SPSS program (IBM, Armonk, NY). Although postmortem intervals (PMIs) among AD cases and controls were comparable ($p = 0.450$), we repeated the analyses including PMI as a covariate, because differences in PMI can affect brain biochemistry and quality of RNA. Because results from models with and without PMI were similar, we reported only the results without adjustment for PMI.

Results

Genome-Wide Association

The mean onset age of AD among the 61 incident cases in the FHS data set was about 10 years older than that for the 1,819 AD cases in the NIA-LOAD data set (Table 1). The frequency of *APOE* ε4 carriers in affected subjects was approximately 2× greater in the NIA-LOAD cohort compared to the FHS cohort. In addition, the proportion of *APOE* ε4 carriers in controls was 15% less in the FHS cohort. Among the 1,969 unaffected family members in the NIA-LOAD cohort, 439 had propensity scores of at least 80% (ie, risk to develop AD accounting for parental affection status and age at onset/examination) and 809 had propensity scores of zero, indicating true controls.

Analysis of genotyped SNPs (n = 341,492 post-QC) in the FHS data set using the normalized liability scores for AD (Fig 1A) indicated little genomic inflation ($\lambda = 1.01$, see Fig 1B), with strong evidence of association in 3 regions of the genome (see Fig 1C). Genome-wide significant associations were found with SNPs in *ITIH3* (rs9311482: $\beta = 1.3$, $p = 5 \times 10^{-9}$), *PLXNA4* (rs277484: $\beta = 1.1$, $p = 9 \times 10^{-10}$), and *MYO18B* (rs13057714: $\beta = 1.0$, $p = 9 \times 10^{-9}$). SNPs located in *IGSF21* were suggestive at $p < 10^{-6}$ (Supplementary

TABLE 1. Sample Characteristics

Characteristics	Family Set		ADGC Set		
	FHS	NIA-LOAD	Caucasian	African American	Japanese
Total, No.	2,876	3,828	18,901	4,896	1,845
AD Cases, No.	61	2,530	9,966	1,459	951
Female, %	54	63	58	70	64
Age at onset for AD cases, yr, mean (SD)	82.8 (9.2)	73.3 (7.0)	76.4 (8.4)	79.4 (7.7)	73.0 (4.3)
Age at last examination for AD controls, yr, mean (SD)	68.1 (10.6)	75.4 (11.6)	77.3 (7.7)	77.4 (8.2)	76.9 (6.0)
% of *APOE* ε4-carriers in cases	42.6	75.0	56.0	57.3	56.3
% *APOE* ε4-carriers in controls	21.6	36.6	21.5	34.7	15.9

The ADGC replication set consisted of previously reported unrelated data sets from 14 Caucasian studies (excluding NIA-LOAD), 7 African American data sets (excluding NIA-LOAD), and 1 Japanese data set.
AD = Alzheimer disease; ADGC = Alzheimer's Disease Genetics Consortium; *APOE* = apolipoprotein E; FHS = Framingham Heart Study; NIA-LOAD = National Institute on Aging–Late-Onset Alzheimer Disease; SD = standard deviation.

Table 1). Each dose of the minor alleles for these SNPs increased AD liability by at least 1 rank unit (mean liability on the normalized scale). Based on an ad hoc power calculation using the sibling correlation of 0.2 derived from the data, the observed effect sizes and minor allele frequencies (MAFs), and a genome-wide significance level of 1.46×10^{-7}, the FHS data set had between 60% and 95% power to obtain these results even for infrequent SNPs ($0.01 < \text{MAF} < 0.05$; Fig 2). Among the previously known genes for AD, 1 genotyped SNP in *BIN1* was moderately associated with the liability score (rs10180840, $p = 1.4 \times 10^{-4}$). We attempted to discover additional association signals in *IGSF21*, *ITIH3*, *PLXNA4*, and *MYO18B* by evaluating 1,515 genotyped and accurately imputed SNPs ($R^2 \geq 0.8$) in the FHS data set (Supplementary Table 2). *PLXNA4* SNPs rs277470, rs277472, rs277476, and rs277484 were significant ($p < 10^{-9}$ for each, Fig 3A) and in complete linkage disequilibrium (LD) with each other (Fig 4). Among the top *PLXNA4* SNPs, only rs277484 was genotyped. No additional SNPs from the *IGSF21*, *ITIH3*, or *MYO18B* met the significance threshold of 1.4×10^{-7}. The dose of *APOE* ε4 alleles was not significantly associated with the AD liability score in FHS ($p = 0.24$), perhaps because most of the incident cases in this cohort were observed at ages where the ε4 association with AD is relatively weak.[3]

Replication and Extended Analysis of PLXNA4

Next, we tested association of 746 genotyped and accurately imputed SNPs ($R^2 \geq 0.8$) from *PLXNA4* in the NIA-LOAD data set (see Fig 3B), but were unable to replicate any of the top-ranked SNPs obtained in the FHS sample (Supplementary Table 3). However, 16 of the 746 *PLXNA4* SNPs showed significant association at $p < 10^{-3}$ in a model using the normalized liability score, and these association signals were improved using the normalized propensity score (see Supplementary Table 3). We observed an association trend in the same effect direction with rs277470 in NIA-LOAD using the propensity score (p value: FHS = 2.1×10^{-10}, NIA-LOAD = 0.06, meta-analysis = 4.1×10^{-8}; see Fig 3C). Each dose of the minor allele *C* for rs277470 increased the liability rank by at least 1 unit in the FHS data set and the propensity rank by 13% in NIA-LOAD (Table 2). The most significant finding in NIA-LOAD (see Fig 3B) was obtained with genotyped SNP rs12539196 (p value: FHS = 0.114, NIA-LOAD = 3.7×10^{-5}, meta-analysis = 2.8×10^{-5}). The minor allele *C* for rs12539196 decreased the liability rank by 0.09 in FHS and accounts for a 15% reduction in the propensity rank in NIA-LOAD (see Table 2). The result for rs12539196 in the NIA-LOAD data set was not meaningfully changed after adjustment for the number of *APOE* ε4 alleles ($p = 2.7 \times 10^{-5}$) and remained significant after correction for multiple testing ($p = 0.0036$).

Further scrutiny of the *PLXNA4* findings revealed that the most significant SNPs in each data set are clustered in 2 distinct regions between recombination hot spots, are separated by approximately 78,240 base pairs in intron 2 of the largest transcript (TS1), and flank an alternatively spliced exon present only in a much shorter

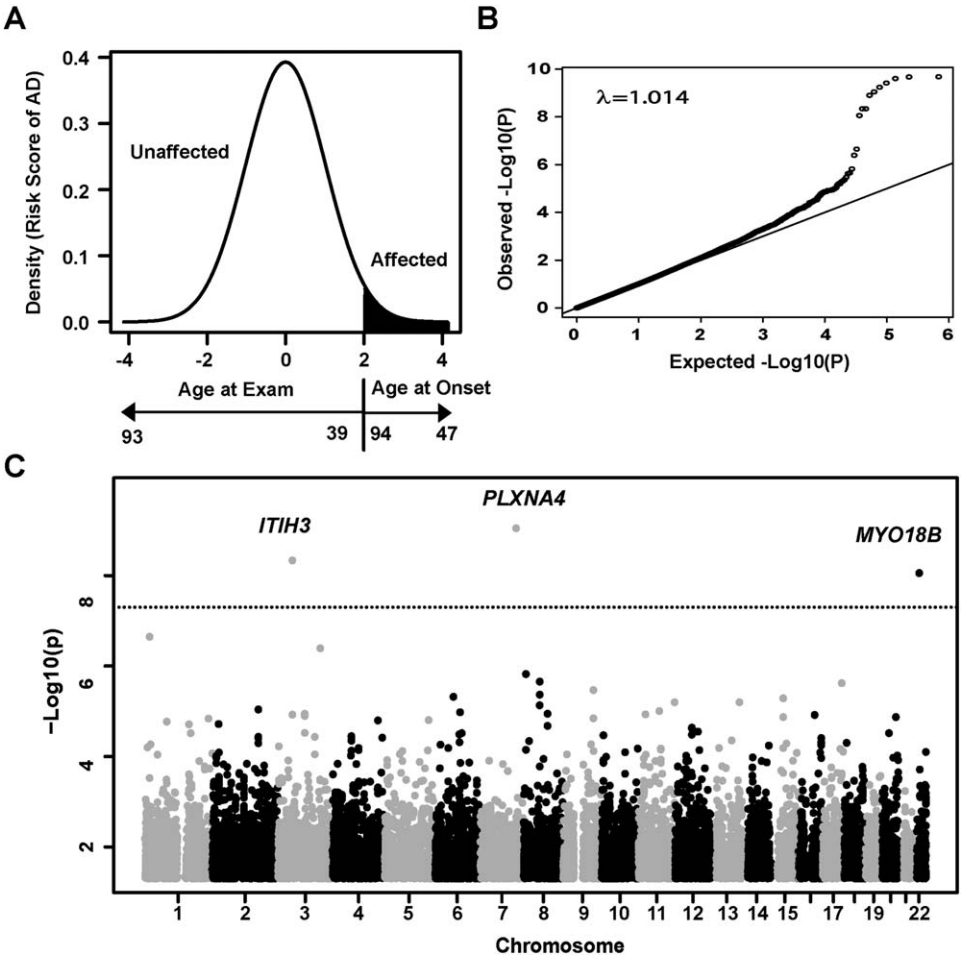

FIGURE 1: Genome-wide association analysis in the Framingham Heart Study. (A) Ranked risk score distribution. Liability scores after adjusting for age and sex in a logistic regression model were rank-transformed and analyzed as a quantitative trait. Shaded area indicates distribution of risk (liability) rank of Alzheimer disease (AD) cases based on age at onset. Arrows for age at examination for controls and for age at onset for AD cases indicate ranks of risk scores. The curve shows that younger unaffected subjects have a higher risk of developing AD than older unaffected subjects, and AD cases with earlier onset have greater liability than cases with older onset. (B) Quantile–quantile plot. Observed probability values (y-axis) were plotted against expected probability values (x-axis). Dots represent probability values for all genotyped single nucleotide polymorphisms (SNPs). (C) Manhattan plot. Association results for genotyped SNPs are shown. Probability values are expressed as $-\log_{10}(p)$ (y-axis) for every tested SNP ordered by chromosomal location (x-axis). Genome-wide significance level is shown as a dotted line at $p = 1.4 \times 10^{-7}$.

transcript (TS3; see Fig 3). Bioinformatic evaluation revealed that TS1 contains a transmembrane domain, whereas the shorter isoforms are predicted to be secreted, suggesting that the longer and shorter isoforms may have distinct functional consequences related to AD. Based on this information, we performed region-based analyses including only SNPs located between 131,925,825 and 132,193,452 base pairs (including all of intron 2) encompassing the SEMA domain, and confirmed significant association for the region (see Table 2) in both data sets (p value: FHS = 6.3×10^{-3}; NIA-LOAD = 0.019; meta-analysis = 3.2×10^{-4}).

Association with *PLXNA4* was further examined using meta-analyzed results in the ADGC data sets. The most significant SNPs in each population under the additive model were rs10273901 in Caucasians (MAF = 0.42; meta-analysis p value [meta-P] = 3.9×10^{-5}; odds ratio [OR] = 0.85, 95% confidence interval [CI] = 0.79–0.92), rs75460865 in African Americans (MAF = 0.04; meta-P = 8.0×10^{-4}; OR = 1.55, 95% CI = 1.20–2.01), and rs13232207 in Japanese (MAF = 0.19; $p = 1.2 \times 10^{-4}$; OR = 1.51, 95% CI = 1.22–1.86). The results for the Caucasian and Japanese groups remained significant after correcting for multiple testing ($p = 0.013$ and $p = 0.037$, respectively). rs75460865 is located in the portion of the sequence that encodes the SEMA domain, but rs10273901 and rs13232207 are located in the *PLXNA4* region that encodes the CYTO domain (see Fig 3E). Top-ranked SNPs in the FHS and NIA-LOAD data sets were not

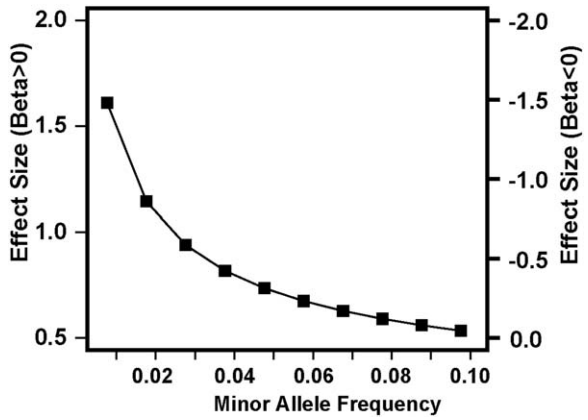

FIGURE 2: Power to detect genome-wide significant association with Alzheimer disease (AD) in the Framingham Heart Study. Effect sizes (ie, beta estimates in the regression model) to obtain 80% power for infrequent single nucleotide polymorphisms (SNPs; 0.01 ≤ minor allele frequency [MAF] ≤ 0.1) under the additive model were estimated using a sibling correlation of 0.199 in 2,779 relative pairs at the genome-wide significance level. Effect size of the SNP on AD risk (y-axis) according to MAF (x-axis) was computed for rank-transformed liability scores. The power estimates are conservative, because they account for only sib-pair relationships in the pedigree.

associated in the other ADGC data sets ($p > 0.1$), likely because power to detect association with several SNPs (including rs277470) having low minor allele frequencies is weaker in the ADGC data sets compared to large extended family-based samples. Because the LD structure in this region is similar across populations (see Fig 4), different association peaks among these groups is consistent with the existence of multiple distinct functionally relevant AD-related alleles. In summary, the results in each of the ADGC ethnic samples support the association of AD with *PLXNA4* SNPs.

PLXNA4 Does Not Influence APP Processing or Aβ Production

To determine whether PLXNA4 isoforms are differentially involved in APP processing and Aβ production, we transfected HEK293 cells stably expressing APP751 with EV control or with the full-length (TS1) or 1 of the shorter isoforms (TS2 and TS3) of PLXNA4-Myc and analyzed total APP in cell lysates, and APPsα, $A\beta_{40}$, and $A\beta_{42}$ in the medium. Neither overexpressing PLXNA4 isoforms affected APPsα secretion (Fig 5A, B) or $A\beta_{40}$ and $A\beta_{42}$ production (see Fig 5C). These results suggest that PLXNA4 is not involved in AD through the nonamyloidogenic or amyloidogenic processing of APP.

PLXNA4 Isoforms Differentially Affect Tau Phosphorylation

Involvement of plexin-A4 signaling in tau phosphorylation was examined by transfecting cDNAs for the full-length (TS1) or 3′ C-terminal truncated short isoforms (TS2 and TS3) of human PLXNA4-Myc into SH-SY5Y P301L cells (SH-SY5Y cells stably expressing the P301L tau mutant) and stimulated with or without 3nM recombinant Sema3A-FC. Immunoblotting with AT8 (anti-phospho-Tau at Ser^{202}/Thr^{205}) showed that tau phosphorylation was induced by SEMA3A stimulation, which was enhanced by overexpression of TS1 (Fig 6A). In contrast, overexpression of either TS2 or TS3 inhibited tau phosphorylation under stimulation by SEMA3A. Because TS2 and TS3 are secretory molecules with the SEMA3A binding site in the extracellular domain, we assume that the inhibitory effect is mediated by the competitive binding of the short isoforms to SEMA3A. Pull-down assays confirmed that the short isoforms, but not full-length PLXNA4, specifically coprecipitated with SEMA3A in the media (see Fig 3B). These data demonstrate that the short isoforms are secreted as expected and bind to SEMA3A, thereby inhibiting signaling. To confirm that SEMA3A/PLXNA4 signaling phosphorylates endogenous wild-type tau protein, we repeated the experiment in rat primary hippocampal neurons. That SEMA3A activated PLXN signaling, leading to phosphorylation of endogenous CRMP2 at Thr^{514} by glycogen synthase kinase-3β, was confirmed in the primary cultured hippocampal neurons (see Fig 6C). Stimulation of neurons with SEMA3A induced phosphorylation of endogenous tau as determined by $AT8^+$ cells (see Fig 6D, red staining in Myc^- cells). Transient expression of Myc-tagged full-length PLXNA4 significantly elevated SEMA3A-induced endogenous tau phosphorylation (Myc^+AT8^+ cells) as compared to untransfected neurons (Myc^- $AT8^+$ cells, $p < 0.01$), whereas expression of Myc-tagged shorter isoforms significantly reduced SEMA3A-induced tau phosphorylation in neuron. This demonstrates that SEMA3A/PLXNA4 signaling phosphorylates endogenous tau in an isoform-specific manner.

Expression of PLXNA4 in Brain Is Different in AD Cases and Controls

Expression of the TS1 and TS3 was quantified in brain tissue specimens from the middle frontal gyrus (Brodmann area 9) from 19 autopsied subjects, including 5 controls, 5 early stage AD cases, and 9 late stage AD cases (Supplementary Table 4) using the primer sets shown in Supplementary Table 5. Late stage AD cases compared to controls had 1.9-fold increased expression of TS1 ($p = 6.0 \times 10^{-4}$) and a more modestly increased expression of TS3 ($p = 0.021$) and ratio of TS1/TS3 ($p = 0.066$; Fig 7). These patterns were similar in the comparison of all AD cases to controls (p-value: TS1 = 0.003, TS3 = 0.097, TS1/TS3 = 0.18) and are

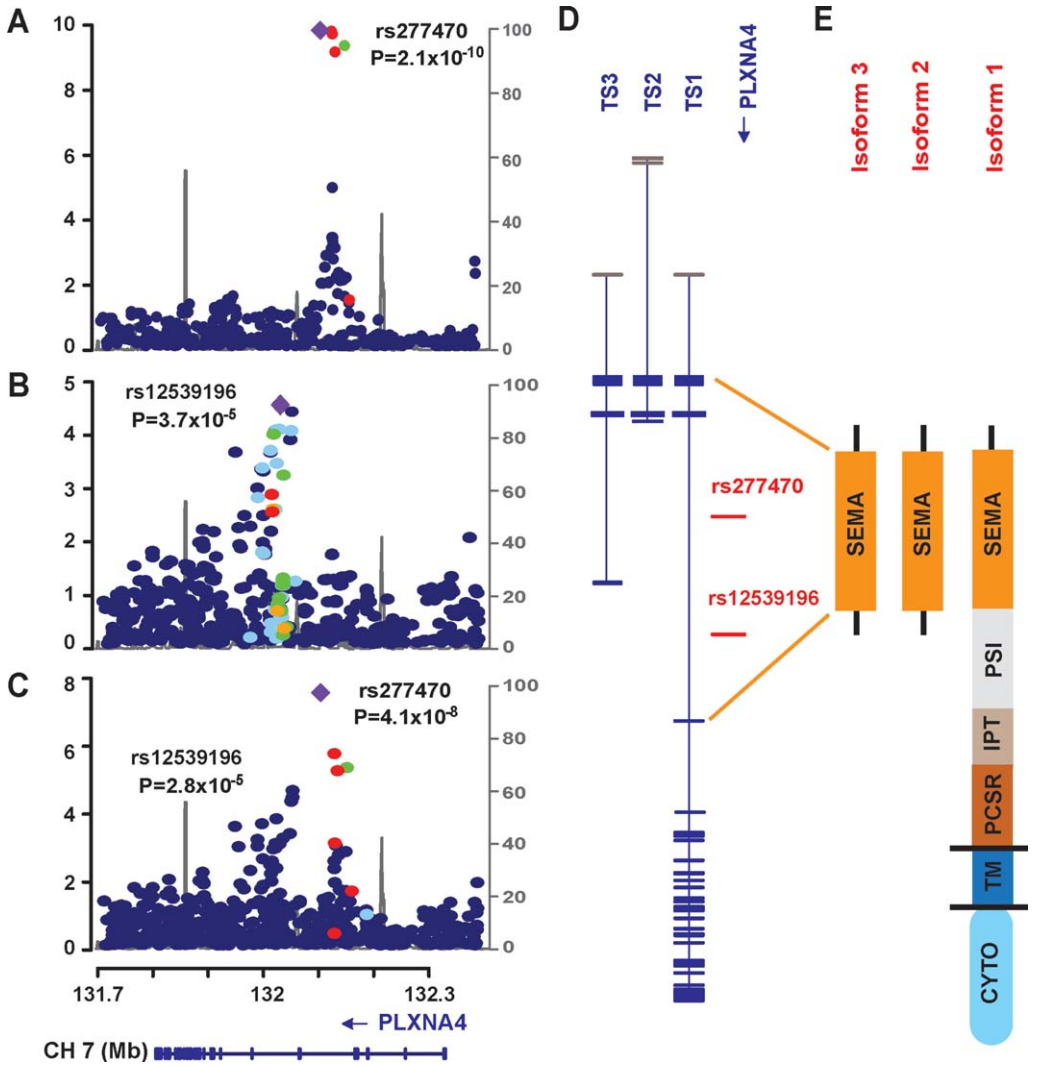

FIGURE 3: Genetic findings in the *PLXNA4* region. (A–C) Regional association plots of genotyped and imputed SNPs from the Framingham Heart Study (FHS; A) and National Institute on Aging–Late-Onset Alzheimer Disease (NIA-LOAD; B) data sets, and in meta-analysis (C). Most significant single nucleotide polymorphisms (SNPs) in the FHS (rs277470) and NIA-LOAD (rs12539196) data sets are indicated by purple diamonds. Probability values are expressed as $-\log_{10}(p)$ (y-axis) for every tested SNP ordered by chromosomal location (x-axis). Estimates of linkage disequilibrium (r^2) of SNPs in this region with the top SNP computed using 1000 Genomes (hg19/Nov2010EUR) are shown as red circles for $r^2 \geq 0.8$, yellow circles for $0.5 \leq r^2 < 0.8$, light blue circles for $0.2 \leq r^2 < 0.5$, and blue circles for $r^2 < 0.2$. Recombination rates (scale on right axis) are plotted with a solid gray line. Genomic structure of *PLXNA4* was determined using the National Center for Biotechnology Information database (Build 37.1). (D) Relative position of the most significantly associated SNPs in the FHS and NIA-LOAD data sets in the 3 validated transcripts (TS1, TS2, and TS3). Exons are denoted with horizontal bars. (E) Diagrams of functional domains encoded by amino acids from the full-length (TS1) and the shorter (TS2 and TS3) transcripts. CYTO = cytoplasmic domain (exons 20–31 in TS1); IPT = 3 repeats of the binding domains of plexins and cell surface receptors (exons 11–17 n TS1); PCSR = binding domain of plexins and cell surface receptors and related proteins (exons 17–19 in TS1); PSI = plexin repeat (exons 4–11 in TS1); SEMA = sema_plexinA1-interacting module (exons 1–4 in TS1 and exons 1–3 in TS2 and TS3); TM = transmembrane region (exon 19 in TS1).

not age-related (Table 3). In the combined sample of AD cases and controls, TS1 level was significantly correlated with the clinical dementia rating score ($\rho = 0.75$, $p = 2.2 \times 10^{-4}$) and several measures of AD neuropathology ($\rho \approx 0.5$, $p < 0.05$), but the correlations of TS3 level with these traits were much smaller (see Table 3). These findings suggest that elevation in TS1 level increases risk for developing AD.

Discussion

We identified significant association between AD risk and SNPs in *PLXNA4* using a family-based approach. The top-ranked SNPs in the discovery and replication data sets are located in a single intron and surround an exon that is skipped in the processing of the full-length mRNA transcript. We also demonstrated that the full-length isoform (TS1), but not the shorter isoforms (TS2

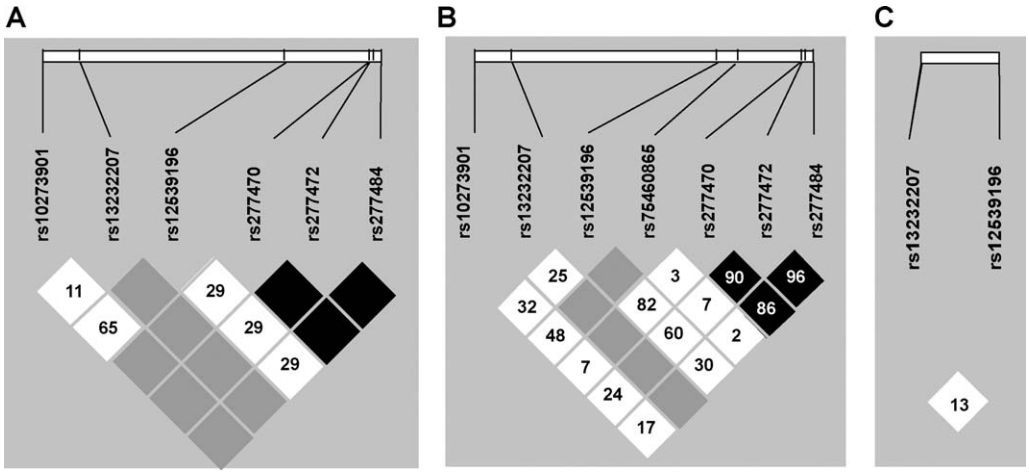

FIGURE 4: Linkage disequilibrium (LD) of top-ranked single nucleotide polymorphisms (SNPs). LD was calculated in 1000 Genomes data from (A) Caucasians (CEU), (B) African Americans (AA), and (C) Asians (ASN). Top-ranked SNPs from *PLXNA4* from each data set are shown, namely rs277470, rs277472, and rs277484 in Framingham Heart Study; rs12539196 in National Institute on Aging–Late-Onset Alzheimer Disease, rs10273901 in Alzheimer's Disease Genetics Consortium (ADGC) Caucasians, rs75460865 in ADGC African Americans, and rs13232207 in ADGC Japanese. The top SNP in the ADGC-AA data set was monomorphic in both CEU and ASN populations. Five top-ranked SNPs (rs10273901, rs75460865, rs277470, rs277472, and rs277484) from the ADGC-CEU and ADGC-AA samples were monomorphic in the ASN population. The top-ranked SNPs are located in the SEMA domain, except for rs10273901 and rs13232207, which are located in the cytoplasmic domain.

and TS3) of PLXNA4 increased tau phosphorylation in SH-SY5Y cells stably expressing the P301L tau mutant and in primary rat neurons when stimulated by SEMA3A. Significantly higher levels of TS1 and TS3 in cortical brain tissue were observed in late stage AD cases compared to controls. By comparison, transfection of either isoform into HEK293 cells stably expressing APP failed to show differential effects on APP processing or Aβ production. Taken together, our results indicate that PLXNA4-mediated tau phosphorylation is an independent upstream event leading to AD-related tangle formation in neurons.

PLXNA4 is a member of a family of receptors for transmembrane, secreted, and glycosylphosphophatidylinositol-anchored semaphorins in vertebrates[31] and is a receptor for secreted SEMA3A and SEMA6 proteins, which play an important role in semaphorin signaling and axon guidance.[32] Accumulation of SEMA3A was previously detected in susceptible areas of the hippocampal neurons during AD progression and colocalized with phosphorylated tau.[33] A phosphorylated CRMP2 protein, an intracellular signaling molecule for the semaphorin–plexin signaling pathway, has been observed in neurofibrillary tangles in brains of autopsied AD

TABLE 2. Top-Ranked SNP-Based Association Results for *PLXNA4* in the FHS and NIA-LOAD Data Sets

SNP or Region	BP	RA	FHS			NIA-LOAD			Meta-Analysis	
			RAF	β^a	p	RAF	β^a	p	Z^b	p
rs277470	132,110,922	C	0.01	1.15	2.1×10^{-10}	0.01	0.13	0.0616	5.49	4.1×10^{-8}
rs12539196	132,037,683	A	0.84	0.09	0.114	0.85	0.15	3.7×10^{-5}	4.19	2.8×10^{-5}
SEMA Region[c]	131,925,825–132,193,452	nSNP = 246			6.3×10^{-3}	nSNP=240		0.019	3.60	3.2×10^{-4}

[a]Estimate of effect size.
[b]Z score in meta-analysis.
[c]Region-based test was conducted using all SNPs from 131,925,825 to 132,193,452 base pairs flanking exons 1 to 3 from three transcript isoforms on chromosome 7.
BP = map position in base pairs from CRCh37/hg19; FHS = Framingham Heart Study; NIA-LOAD = National Institute on Aging–Late-Onset Alzheimer Disease; nSNP = number of SNPs in a region-based test; RA = reference allele; RAF = reference allele frequency; SNP = single nucleotide polymorphism.

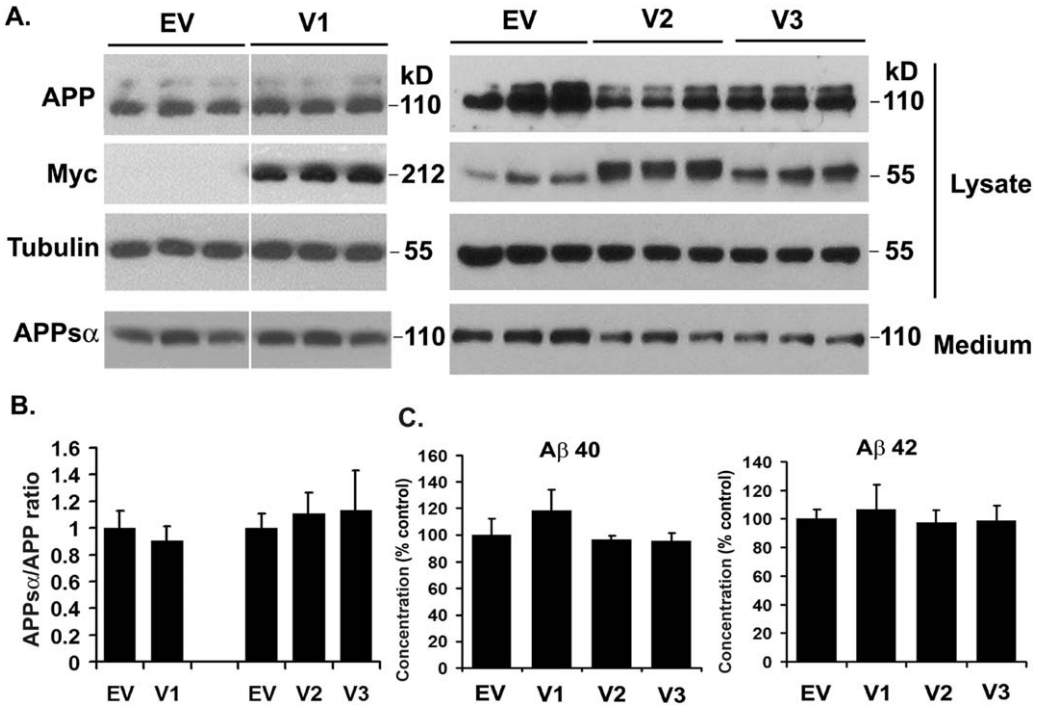

FIGURE 5: Effect of expression of the full-length PLXNA4 isoforms (TS1, TS2, and TS3) on amyloid β (Aβ) precursor protein (APP) processing. HEK293 cells stably overexpressing APP were transiently transfected with empty vector control (EV) or with the full-length (TS1) or 1 of the shorter isoforms (TS2 and TS3) of PLXNA4-Myc. (A) Forty-eight hours after transfection, the conditioned medium (Medium) and the cell lysates (Lysate) were collected and analyzed by sodium dodecyl sulfate–polyacrylamide gel electrophoresis and Western blotting using monoclonal antibod 6E10 for total APP and APPsα, Myc mAb for all 3 isoforms of PLXNA4, and tubulin as control. The endogenous myc can be seen in all lanes at ~55kDa but more clearly in lanes 7 to 9, where only empty vector was transfected but not PLXNA4-myc. Also note that TS1 migrates at 212kDa, TS2 migrates at 58kDa, and TS3 migrates at 55kDa. (B) Densitometric analysis of the expression of APPsα normalized to total APP. Error bars indicate standard deviation. (C) Enzyme-linked immunosorbent assay (ELISA) analysis of Aβ_{40} and Aβ_{42} released to the medium. ELISAs were carried out using the human Aβ_{40} and Aβ_{42} ELISA kits (Invitrogen) in accordance with the manufacturer's protocol. Error bars indicate standard deviation. Representative results of 3 independent experiments are shown in each panel.

patients.[34] The staining pattern of SEMA6, which is present in fibers and nerve terminals, is disrupted in brains of patients with AD.[35] These reports and our study collectively indicate that disrupted semaphorin–plexin signaling is involved in AD pathogenesis, specifically through tau phosphorylation leading to tangle formation and neuronal death. Semaphorin–plexin signaling is known to regulate axon guidance in the development of sympathetic nervous system and cerebral cortex.[36–38] Binding of SEMA3A to truncated PLXNA proteins was demonstrated to have a dominant negative effect on cortical growth cone collapse.[39] Our data indicate that disruption of this signaling may also contribute to the acceleration of tau phosphorylation leading to neurofibrillary tangle formation. A recent whole exome sequence study identified a rare coding *PLXNA4* variant in 2 distantly related individuals with familial Parkinson disease (PD).[40] Notably, both PD subjects were cognitively impaired and there is a recognized form of PD with dementia. Further screening of all *PLXNA4* exons in a large sample of unrelated PD cases and controls revealed a large number of very rare coding variants unique to cases or controls. Although the pathogenicity of these variants is yet unknown, this study provides additional evidence supporting *PLXNA4* as a common biological pathway leading to AD and PD. Taken together, our findings point to a novel mechanism for AD-related tangle formation, implying that reduced expression of *PLXNA4*, and the TS1 isoform in particular, in brain is crucial to maintain healthy neurons.

There are 3 known alternatively spliced *PLXNA4* transcripts. The full-length transcript (TS1) contains 31 exons and encodes an isoform with 1,894 residues. Two alternatively spliced transcripts each contain 3 exons yielding shorter isoforms of 522 residues (TS2) and 492 residues (TS3). The distinct *PLXNA4* association peaks in the discovery and replication data sets flank an exon that is present only in TS3. A direct link of *PLXNA4* expression to AD is supported by evidence in this report of increased expression of TS1 and TS3 isoforms in

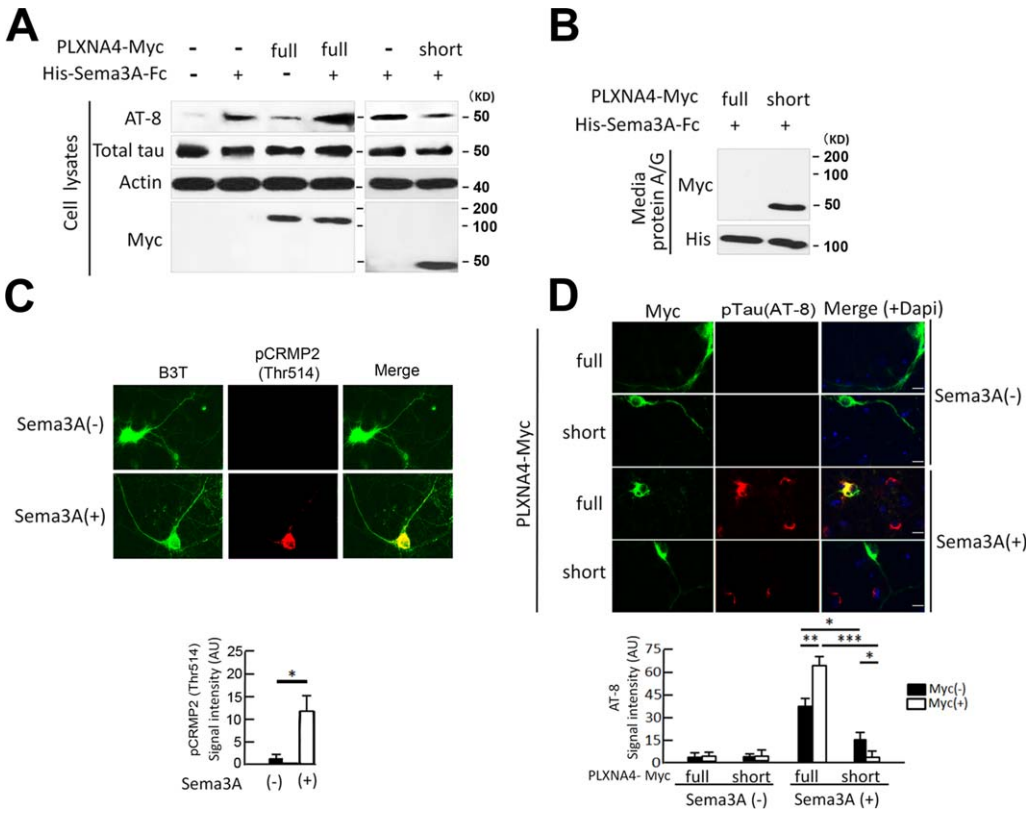

FIGURE 6: Effect of PLXNA4 isoforms on tau phosphorylation. (A) SH-SY5Y P301L cells were transfected with the full-length (TS1) or 1 of the shorter isoforms (TS2 and TS3) of PLXNA4-Myc or empty vectors (pcDNA3.1) with or without 3nM SEMA3A stimulation for 1 hour. Whole cell lysates were blotted with AT8, total tau, actin and Myc. Results for the TS2 and TS3 isoforms were similar, but only those for TS3 are shown. (B) 6xHis-tagged SEMA3A-Fc was precipitated from media by protein A/G agarose, and the precipitates were immunoblotted with antibodies to Myc (detecting PLXNA4 isoforms) and 6xHis (detecting SEMA3A-FC). (C) Embryonic day 18 rat primary hippocampal neurons were cultured for 14 days and stimulated with 3nM SEMA3A for 1 hour, and costained with anti-β3-tubulin (B3T) mouse monoclonal (1:500, green) and anti-pT514 CRMP2 rabbit polyclonal antibody (1:500, red). (D) Rat primary hippocampal neurons were transfected with the full-length or short isoforms of plexin-A4-Myc. After transfection, cells were treated with or without 3nM Sema3A for 1 hour, and costained with AT8 (1:500) and anti-Myc (rabbit polyclonal, 1:200; Covance). AT8 signals were digitally captured and quantified as previously reported.[47] Cells are immunostained with anti-Myc (green) and AT8 (red). Scale bars = 10μm. *$p<0.05$, **$p<0.01$, ***$p<0.001$, as determined by analysis of variance and Tukey post hoc test.

postmortem neuronal tissue from AD cases compared to controls. Importantly, the findings that the relative increase of TS1 is much greater than TS3 in AD cases, and TS1 expression is significantly correlated with clinical and neuropathological severity measures of AD, are consistent with our observation of increased phosphorylation of tau by SEMA3A bound specifically to TS1.

Previous GWASs involving the FHS data set have successfully identified several AD genes, including *BIN1, MS4A4/MS4A6A, EPHA7, ABCA7, CD33, CD2AP, HLA-DRB5–HLA-DRB1, PTK2B, SLC24A4-RIN3, INPP5D, MEF2C, NME8, ZCWPW1, CELF1, FERMT2,* and *CASS4*,[4,16,41] but the portion of evidence for these associations attributable to the FHS data set is very small, and the robust associations with these loci are with common SNPs (MAF >0.08) each exerting a small effect on risk (OR ≤ 1.2). We increased the potential for gene discovery in the FHS and NIA-LOAD data sets by applying an analytical method that leverages the family structure that is otherwise ignored when using Generalized Estimating Equations models. Our approach is applicable to extended pedigrees and is robust for detecting association with infrequent SNPs ($0.01 \leq$ MAF < 0.1), because the power for this method is largely dependent on effect size rather than allele frequencies.[11] Except for *BIN1*, lack of significant associations with most of the previously known AD loci suggests that they do not contain large effect variants for AD risk in the range of infrequent MAFs. In addition, we addressed phenotype misclassification by including only incident cases with known onset ages in the FHS data set and by using the propensity score approach in the NIA-LOAD data set, which has a skewed distribution of onset ages and is enriched with familial AD cases. Our method using propensity scores as a surrogate for AD susceptibility assigned probabilities >50% for future

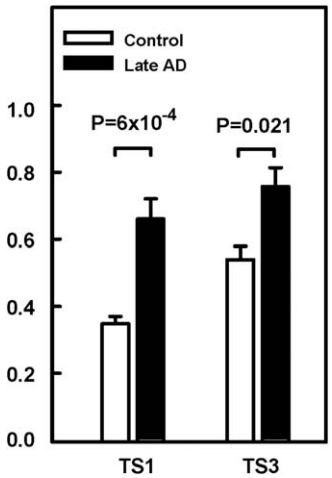

FIGURE 7: Expression of *PLXNA4* isoforms in postmortem brains. Expression of *PLXNA4* isoforms from Brodmann area 9 of frozen postmortem brain tissue specimens were compared in controls and late stage Alzheimer disease (AD) cases using primer sets to detect full-length (TS1) and short (TS3) isoforms. RNA expression level (y-axis) shown is the normalized value. Probability values were determined by *t* test accounting for unequal variances.

development of AD to 60% of the unaffected subjects at last examination in the NIA-LOAD cohort. This indicates that analyses using affection status in families with multiple affected members have much less power to detect true associations without adjusting for misclassification of unaffected relatives.

Our study has several caveats. Power to detect association with AD risk is low in the FHS cohort because of the small number of incident cases. We overcame this limitation by using a continuous measure of AD liability instead of AD status as the outcome. In addition, the top-ranked *PLXNA4* SNPs were not the same across data sets, and thus the lack of an exact replication may indicate that the initial finding was a false positive. However, the inability to replicate at the SNP level can be explained by differences in allele frequencies across populations, and low power and reliability to detect association with infrequent SNPs in samples of unrelated cases and controls. Another likely contributor to the different association patterns is allelic heterogeneity, which we observed for *SORL1*[42] and has been reported among Caucasians for other common diseases.[43,44] Nevertheless, our *PLXNA4* region-based test results were significant in both the FHS and NIA-LOAD data sets. Moreover, the observed effects of PLXNA4 isoforms on AD-related processes in cultured neuronal cells and brain, which were identified through experiments conducted because of the association findings, suggest that the significant results with individual *PLXNA4* SNPs are not false positives. Another concern is that we did not have genotypes for the top-ranked SNPs in a large sample of AD cases and controls with brain tissue available for study. As a result, we were unable to investigate allele-specific effects on isoform expression levels. Moreover, demonstration of higher isoform levels in peripheral tissue of living AD cases compared to controls would lessen the concern that the differences observed in brain are not secondary to underlying pathology. In addition, in vitro tau phosphorylation experiments do not indicate which tau kinases activate tau phosphorylation. Cyclin-dependent kinase 5 and glycogen synthase kinase-3β are known to be activated by SEMA3A by phosphorylating CRMP2 to mediate growth cone collapse.[45,46] It is most likely that PLXNA4 induces tau phosphorylation via activation of these 2 established kinases. Also, because these results are based on the transient expression of PLXNA4 molecules, it is crucial to evaluate the influence of PLXNA4 on tau phosphorylation in more physiological conditions. Isoform-specific targeting of *PLXNA4* in mice is a potential future study in vivo.

In summary, our novel genetic association findings and results of molecular and cell biology experiments in cell lines, rat neurons, and human brain demonstrate that *PLXNA4* is involved in AD pathogenesis. Evidence supporting transcriptional regulation of *PLXNA4* isoforms that have differential effect on tau phosphorylation and hence tangle formation suggests the potential for a

TABLE 3. Correlation of PLXNA4 Isoform Levels with Clinical and Neuropathological Phenotypes in Brain Specimens from Subjects with Alzheimer Disease and Controls

Characteristics	Correlation (*p*)	
	TS1	TS2
Age	0.27 (0.27)	0.31 (0.20)
PMI	−0.01 (0.97)	0.35 (0.14)
RIN	−0.09 (0.70)	−0.35 (0.14)
CDR	0.75 (2.2×10^{-4})	0.56 (0.014)
Plaque BM9[a]	0.47 (0.045)	0.24 (0.32)
Plaque mean[b]	0.56 (0.012)	0.36 (0.13)
Braak stage	0.54 (0.017)	0.55 (0.015)

[a]Neuritic plaque density Brodmann area 9.
[b]Mean of plaque densities measured in 5 cortical regions including Brodmann area 9 (middle frontal gyrus), Brodmann area 45/47 (orbital frontal gyrus), Brodmann area 21/22 (superior temporal gyrus), Brodmann area 39 (inferior parietal cortex), and Brodmann area 17 (calcarine cortex).
CDR = Clinical Dementia Rating; PMI = postmortem interval; RIN = RNA integrity number.

new drug target. These findings warrant follow-up experiments to delineate the upstream factors governing PLXNA4 binding to CRMP2, ascertain the causative genetic variants at the 2 association peaks and determine how they modulate expression of the individual isoforms, demonstrate in brain tissue that the genetic variation in *PLXNA4* is associated with AD risk or progression, and evaluate the utility of PLXNA4 as a potential biomarker for AD. Further studies of PLXNA4 may also provide mechanistic evidence linking AD to PD with comorbid dementia.

Acknowledgment

Supported by grants from the NIH National Institute on Aging (R01-AG025259, PG30-AG13846, R01-AG0001, U24-AG021886, U24-AG26395, R01-AG041797, and P50-AG005138), the Brain Research Program through the National Research Foundation of Korea, funded by the Ministry of Science, ICT, and Future Planning (NRF-2013M3C7A1073000), the Evans Center for Interdisciplinary Biomedical Research (ECIBR) Affinity Research Collaborative on "Protein Trafficking and Neurodegenerative Disease" at Boston University (http://www.bumc.bu.edu/evanscenteribr/), and Grant-in-Aid for Scientific Research on Innovative Areas (R.K.). G.J. was supported by an ECIBR Fellowship Award. The results of this study were obtained using the Boston University Linux Cluster for Genetic Analysis (LinGA), which was established with support from U.S. Public Health Service Resource Grant RR163736 from the National Center for Research Resources and Boston University Department of Medicine. The HEK293 cells stably overexpressing wild-type APP751 were a kind gift from D. J. Selkoe, Harvard Medical School, and the Myc-tagged PLXNA4 (TS1) was a kind gift from Dr. G. Neufeld, Technion, Israel Institute of Technology.

The Framingham Heart Study is conducted and supported by the National Heart, Lung, and Blood Institute (NHLBI) in collaboration with Boston University (contract No. N01-HC-25195). This article was not prepared in collaboration with investigators of the Framingham Heart Study and does not necessarily reflect the opinions or views of the Framingham Heart Study, Boston University, or NHLBI.

We thank Drs. Y. Song and R. C. Elston for their technical help and advice using the S.A.G.E. software package.

Authorship

G.J. designed and performed the genetic association analyses and cowrote the article. J.C. assisted in the genetic association analyses and performed the meta analyses. H.A. performed the tau phosphorylation experiments. E.Z. and C.C. performed the Aβ and APP experiments. E.D. performed the PLXNA4 isoform studies in brain. J.-H.P, S.K., and J.-W.K. designed primer sets and tested the efficacy in blood. T.F. and R.M. ascertained, phenotyped, and genotyped the NIA-LOAD study participants. V.H. obtained and characterized the brain specimens. R.K., M.A.P-V, J.L.H, and G.D.S provided Alzheimer's Disease Genetics Consortium data sets and helped interpret results. K.L.L. consulted on the statistical genetic analyses and critically evaluated the manuscript. J.D.B. supervised the PLXNA4 genotyping and isoform studies in brain and critically evaluated the manuscript. T.I. designed and supervised the tau phosphorylation experiments and assisted in the preparation of the manuscript. C.R.A. designed the Aβ and APP experiments and assisted in the preparation of the manuscript. L.A.F. obtained funding for the study, coordinated all components of the study, evaluated and interpreted results, and cowrote the article.

Potential Conflicts of Interest

G.J., L.A.F.: patent pending, US 61/821,397.

References

1. Thies W, Bleiler L. 2011 Alzheimer's disease facts and figures. Alzheimers Dement 2011;7:208–244.
2. Farrer LA. Genetics and the dementia patient. Neurologist 1997;3: 13–30.
3. Farrer LA, Cupples LA, Haines JL, et al. Effects of age, sex, and ethnicity on the association between apolipoprotein E genotype and Alzheimer disease. A meta-analysis. APOE and Alzheimer Disease Meta Analysis Consortium. JAMA 1997;278:1349–1356.
4. Lambert JC, Ibrahim-Verbaas CA, Harold D, et al. Meta-analysis of 74,046 individuals identifies 11 new susceptibility loci for Alzheimer's disease. Nat Genet 2013;45:1452–1458.
5. Lill CM, Bertram L. Towards unveiling the genetics of neurodegenerative diseases. Semin Neurol 2012;31:531–541.
6. Paulson HL, Igo I. Genetics of dementia. Semin Neurol 2012;31: 449–460.
7. Naj AC, Jun G, Beecham GW, et al. Common variants at MS4A4/MS4A6E, CD2AP, CD33 and EPHA1 are associated with late-onset Alzheimer's disease. Nat Genet 2011;43:436–441.
8. So HC, Gui AH, Cherny SS, Sham PC. Evaluating the heritability explained by known susceptibility variants: a survey of ten complex diseases. Genet Epidemiol 2011;35:310–317.
9. Manolio TA, Collins FS, Cox NJ, et al. Finding the missing heritability of complex diseases. Nature 2009;461:747–753.
10. Sherva R, Farrer LA. Power and pitfalls of the genome-wide association study approach to identify genes for Alzheimer's disease. Curr Psychiatry Rep 2011;13:138–146.
11. Choi SH, Liu C, Dupuis J, et al. Using linkage analysis of large pedigrees to guide association analyses. BMC Proc 2011;5(suppl 9):S79.

12. Cobb JL, Wolf PA, Au R, et al. The effect of education on the incidence of dementia and Alzheimer's disease in the Framingham Study. Neurology 1995;45:1707–1712.
13. Wijsman EM, Pankratz ND, Choi Y, et al. Genome-wide association of familial late-onset Alzheimer's disease replicates BIN1 and CLU and nominates CUGBP2 in interaction with APOE. PLoS Genet 2011;7:e1001308.
14. Miyashita A, Koike A, Jun G, et al. SORL1 is genetically associated with late-onset Alzheimer's disease in Japanese, Koreans and Caucasians. PLoS One 2013;8:e58618.
15. Reitz C, Jun G, Naj A, et al. Variants in the ATP-binding cassette transporter (ABCA7), apolipoprotein E 4,and the risk of late-onset Alzheimer disease in African Americans. JAMA 2013;309:1483–1492.
16. Seshadri S, Fitzpatrick AL, Ikram MA, et al. Genome-wide analysis of genetic loci associated with Alzheimer disease. JAMA 2010; 303:1832–1840.
17. Jun G, Naj AC, Beecham GW, et al. Meta-analysis confirms CR1, CLU, and PICALM as Alzheimer disease risk loci and reveals interactions with APOE genotypes. Arch Neurol 2010;67:1473–1484.
18. Li Y, Abecasis GR. Mach 1.0: rapid haplotype reconstruction and missing genotype inference. Am J Hum Genet 2006;S79:2290.
19. Jun G, Moncaster JA, Koutras C, et al. Delta-catenin is genetically and biologically associated with cortical cataract and future Alzheimer-related structural and functional brain changes. PLoS One 2012;7:e43728.
20. Hanson RL, Knowler WC. Analytic strategies to detect linkage to a common disorder with genetically determined age of onset: diabetes mellitus in Pima Indians. Genet Epidemiol 1998;15:299–315.
21. Jiang Y, Zhang H. Propensity score-based nonparametric test revealing genetic variants underlying bipolar disorder. Genet Epidemiol 2011;35:125–132.
22. Schnell AH, Sun X, Igo RP Jr, Elston RC. Some capabilities for model-based and model-free linkage analysis using the program package S.A.G.E. (Statistical Analysis for Genetic Epidemiology). Hum Hered 2011;72:237–246.
23. Jun G, Guo H, Klein BE, et al. EPHA2 is associated with age-related cortical cataract in mice and humans. PLoS Genet 2009;5: e1000584.
24. Morris NJ, Elston R, Stein CM. Calculating asymptotic significance levels of the constrained likelihood ratio test with application to multivariate genetic linkage analysis. Stat Appl Genet Mol Biol 2009;8:Article 39.
25. Wang T, Elston RC. Two-level Haseman-Elston regression for general pedigree data analysis. Genet Epidemiol 2005;29:12–22.
26. Liu JZ, McRae AF, Nyholt DR, et al. A versatile gene-based test for genome-wide association studies. Am J Hum Genet 2010;87:139–145.
27. Willer CJ, Li Y, Abecasis GR. METAL: fast and efficient meta-analysis of genomewide association scans. Bioinformatics 2010;26: 2190–2191.
28. So PP, Zeldich E, Seyb KI, et al. Lowering of amyloid beta peptide production with a small molecule inhibitor of amyloid-beta precursor protein dimerization. Am J Neurodegener Dis 2012;1:75–87.
29. Sato S, Xu J, Okuyama S, et al. Spatial learning impairment, enhanced CDK5/p35 activity, and downregulation of NMDA receptor expression in transgenic mice expressing tau-tubulin kinase 1. J Neurosci 2008;28:14511–14521.
30. Haroutunian V, Perl DP, Purohit DP, et al. Regional distribution of neuritic plaques in the nondemented elderly and subjects with very mild Alzheimer disease. Arch Neurol 1998;55:1185–1191.
31. Tamagnone L, Artigiani S, Chen H, et al. Plexins are a large family of receptors for transmembrane, secreted, and GPI-anchored semaphorins in vertebrates. Cell 1999;99:71–80.
32. Suto F, Ito K, Uemura M, et al. Plexin-a4 mediates axon-repulsive activities of both secreted and transmembrane semaphorins and plays roles in nerve fiber guidance. J Neurosci 2005;25:3628–3637.
33. Good PF, Alapat D, Hsu A, et al. A role for semaphorin 3A signaling in the degeneration of hippocampal neurons during Alzheimer's disease. J Neurochem 2004;91:716–736.
34. Cole AR, Knebel A, Morrice NA, et al. GSK-3 phosphorylation of the Alzheimer epitope within collapsin response mediator proteins regulates axon elongation in primary neurons. J Biol Chem 2004; 279:50176–50180.
35. Hirsch E, Hu LJ, Prigent A, et al. Distribution of semaphorin IV in adult human brain. Brain Res 1999;823:67–79.
36. Low LK, Liu XB, Faulkner RL, et al. Plexin signaling selectively regulates the stereotyped pruning of corticospinal axons from visual cortex. Proc Natl Acad Sci U S A 2008;105:8136–8141.
37. Sasaki Y, Cheng C, Uchida Y, et al. Fyn and Cdk5 mediate semaphorin-3A signaling, which is involved in regulation of dendrite orientation in cerebral cortex. Neuron 2002;35:907–920.
38. Waimey KE, Huang PH, Chen M, Cheng HJ. Plexin-A3 and plexin-A4 restrict the migration of sympathetic neurons but not their neural crest precursors. Dev Biol 2008;315:448–458.
39. Takahashi T, Fournier A, Nakamura F, et al. Plexin-neuropilin-1 complexes form functional semaphorin-3A receptors. Cell 1999; 99:59–69.
40. Schulte EC, Stahl I, Czamara D, et al. Rare variants in PLXNA4 and Parkinson's disease. PLoS One 2013;8:e79145.
41. Hollingworth P, Harold D, Sims R, et al. Common variants at ABCA7, MS4A6A/MS4A4E, EPHA1, CD33 and CD2AP are associated with Alzheimer's disease. Nat Genet 2011;43:429–435.
42. Rogaeva E, Meng Y, Lee JH, et al. The neuronal sortilin-related receptor SORL1 is genetically associated with Alzheimer disease. Nat Genet 2007;39:168–177.
43. Schulze TG, Detera-Wadleigh SD, Akula N, et al. Two variants in Ankyrin 3 (ANK3) are independent genetic risk factors for bipolar disorder. Mol Psychiatry 2009;14:487–491.
44. Voight BF, Scott LJ, Steinthorsdottir V, et al. Twelve type 2 diabetes susceptibility loci identified through large-scale association analysis. Nat Genet 2010;42:579–589.
45. Arimura N, Menager C, Kawano Y, et al. Phosphorylation by Rho kinase regulates CRMP-2 activity in growth cones. Mol Cell Biol 2005;25:9973–9984.
46. Brown M, Jacobs T, Eickholt B, et al. Alpha2-chimaerin, cyclin-dependent Kinase 5/p35, and its target collapsin response mediator protein-2 are essential components in semaphorin 3A-induced growth-cone collapse. J Neurosci 2004;24:8994–9004.
47. Uchida Y, Ohshima T, Sasaki Y, et al. Semaphorin3A signalling is mediated via sequential Cdk5 and GSK3beta phosphorylation of CRMP2: implication of common phosphorylating mechanism underlying axon guidance and Alzheimer's disease. Genes Cells 2005;10:165–179.